molecules

MDPI

Article

Development of Flow Cytometric Assay for Detecting Papillary Thyroid Carcinoma Related hsa-miR-146b-5p through Toehold-Mediated Strand Displacement Reaction on Magnetic Beads

Yue Wu [1], Jiaxue Gao [2], Jia Wei [1], Jingjing Zhou [1], Xianying Meng [1,*] and Zhenxin Wang [2,*]

[1] Department of Thyroid Surgery, The First Hospital of Jilin University, Changchun 130021, China; wuyuejlu@163.com (Y.W.); weijia@ciac.ac.cn (J.W.); zzzj4679@163.com (J.Z.)
[2] State Key Laboratory of Electroanalytical Chemistry, Changchun Institute of Applied Chemistry, Chinese Academy of Sciences, Changchun 130022, China; gjx@ciac.ac.cn
* Correspondence: mengxiany@jlu.edu.cn (X.M.); wangzx@ciac.ac.cn (Z.W.)

Abstract: In this work, a simple enzyme-free flow cytometric assay (termed as TSDR-based flow cytometric assay) has been developed for the detection of papillary thyroid carcinoma (PTC)-related microRNA (miRNA), hsa-miR-146b-5p with high performance through the toehold-mediated strand displacement reaction (TSDR) on magnetic beads (MBs). The complementary single-stranded DNA (ssDNA) probe of hsa-miR-146b-5p was first immobilized on the surface of MB, which can partly hybridize with the carboxy-fluorescein (FAM)-modified ssDNA, resulting in strong fluorescence emission. In the presence of hsa-miR-146b-5p, the TSDR is trigged, and the FAM-modified ssDNA is released form the MB surface due to the formation of DNA/RNA heteroduplexes on the MB surface. The fluorescence emission change of MBs can be easily read by flow cytometry and is strongly dependent on the concentration of hsa-miR-146b-5p. Under optimal conditions, the TSDR-based flow cytometric assay exhibits good specificity, a wide linear range from 5 to 5000 pM and a relatively low detection limit (LOD, 3σ) of 4.21 pM. Moreover, the practicability of the assay was demonstrated by the analysis of hsa-miR-146b-5p amounts in different PTC cells and clinical PTC tissues.

Keywords: hsa-miR-146b-5p; magnetic beads; flow cytometry; thyroid carcinoma

Citation: Wu, Y.; Gao, J.; Wei, J.; Zhou, J.; Meng, X.; Wang, Z. Development of Flow Cytometric Assay for Detecting Papillary Thyroid Carcinoma Related hsa-miR-146b-5p through Toehold-Mediated Strand Displacement Reaction on Magnetic Beads. *Molecules* **2021**, *26*, 1628. https://doi.org/10.3390/molecules26061628

Academic Editors: Eylon Yavin and Laura Cerchia

Received: 25 January 2021
Accepted: 12 March 2021
Published: 15 March 2021

1. Introduction

MicroRNAs (miRNAs) are single-stranded non-coding RNAs, ranging in length from 19 to 25 nucleotides, which were first unintentionally discovered in *Caenorhabditis elegans* by Lee and colleagues in 1993 [1]. MiRNAs enable regulating the expression of target genes by binding to target messenger RNA (mRNA) and inducing its degradation or translation inhibition [2]. Consequently, miRNAs are involved in the regulation of various biological processes in organisms, such as cell proliferation, differentiation, metabolism, embryogenesis, inflammation, senescence and programmed cell death [3,4]. Recently, massive studies have demonstrated that the abnormal expression of miRNA is closely related to the occurrence and development of human malignant tumors including gastric cancer, liver cancer, breast cancer and thyroid cancer [5]. There is a rapidly increasing demand for miRNA detection [6,7], because miRNA is considered as a novel biomarker for cancer diagnosis, prognostic analysis and molecular targeted drug development. Due to their inherent characteristics including short sequence, low abundance and high sequence similarity among family members, it is difficult to precisely detect and analyze miRNAs in practical samples. Recently, various assays/methods have been developed for the detection of miRNAs, such as Northern blot [8], microarray-based method [9], reverse transcription polymerase chain reaction (RT-PCR) [10], isothermal exponential amplification method (EXPAR) [11] and rolling-circle amplification (RCA) method [12]. Although most of these assays/methods

can be employed to detect miRNAs with high sensitivity and accuracy, they have some drawbacks/limitations, such as the complex design of probe/primer/template sequence, tedious detection steps, long assaying time and requirement of expensive reagents (e.g., enzymes). Therefore, there is still a strong desire to develop a feasible approach with high simplicity for rapid quantification of miRNAs in practical samples.

As a versatile tool, magnetic beads (MBs) have been extensively employed for the purification and quantitative detection of different analytes in complex biological matrices since MBs have several unique advantages including good stability, uniform size distribution, easy functionalization and rapid response to applied magnetic field [13–15]. For instance, Li and colleagues have developed a flow cytometric bead assay for the simultaneous detection of multiple miRNAs through the integration of size-coded MBs with a two-step enzyme-mediated cascading signal amplification [16]. Toehold-mediated strand displacement reaction (TSDR) generally takes place in the case of partially hybridized duplex with an overhanging single-stranded toehold domain containing 5−8 nucleotides, in which the displacement reaction is followed by the formation of the toehold-target duplex [17]. The TSDR is a useful strategy for the construction of analytical assays with good performance because the displacement process is fast, predictable and easy to differentiate the mismatched sequences [18–23]. In addition, MB-assisted TSDR with different detection principles including fluorescent [24,25], photoelectrochemical [22], colorimetric and chemiluminescent [26,27] have been developed for the detection of cancer-related miRNAs.

As the most common type of thyroid cancer, papillary thyroid carcinoma (PTC) has been diagnosed with increasing frequency in recent decades in many developed countries and China. Although up to 90% of patients with PTC at early stage can achieve long-term (more than 5 years) survival, life-long surveillance is required [28–30]. Because of non-total thyroidectomy, the presence of anti-thyroglobulin (Tg) antibodies, and/or lack of iodine avidity, the clinical used gold standard of life-long surveillance of PTC, monitoring serum thyroglobulin (Tg) levels is not suitable for up to 25% of patients with PTC [31]. It has been demonstrated that the occurrence and development of PTC has strong association with high levels of several miRNAs including miR-146b, miR-222, and miR-221 [32–35]. For instance, the family member of miR-146b, hsa-miR-146b-5p exhibits very high expression level in PTC, which can promote the proliferation, migration, invasion and cell cycle progression of PTC cells through the regulation of cell signaling pathways including downregulating the expression of CCDC6 [36], IRAK1 and other PTC-related genes [37,38]. Therefore, hsa-miR-146b-5p can be used as a potential biomarker for the diagnosis of PTC and help us to understand the mechanism of tumor development.

Herein, we proposed an enzyme-free flow cytometric assay (termed as a TSDR-based flow cytometric assay) for the detection of thyroid cancer-associated miRNA, hsa-miR-146b-5p through the combination of MB-based TSDR and flow cytometry fluorescence detection. Taking advantage of the flow cytometry's strong analysis ability (such as high sensitivity and high throughput) and a MB's magnetic separation capacity, the as-proposed flow cytometric assay exhibits high performance compared to other methods, which can be employed to rapidly monitor hsa-miR-146b-5p levels in practical samples including cell lysates and the clinical tissue homogenate of PTC, showing great potential in clinical diagnosis.

2. Materials and Methods

2.1. Materials and Reagents

Oligonucleotides (see Table 1 for details) were synthesized by Sangon Ltd. Co. (Shanghai, China). Dynabeads® M-270 streptavidin modified (M-270 MBs, 2.8 μm) and 5 × banding and washing (B&W) buffer (25 mM Tris-Hcl, 2.5 mM EDTA, 5 M NaCl, pH 7.5) were obtained from Thermo Fisher Scientific Co. (Asheville, NC, USA). Diethylpyrocarbonate-treated distilled water (DEPC water) was supplied by Dingguo Biotechnology Ltd. (Beijing, China). All buffers were prepared with DEPC water to prevent miRNA degradation. Dulbecco's modified Eagle's medium (DMEM), RPMI-1640 medium and fetal bovine

serum (FBS) were purchased from HyClone Co. (Los Angeles, CA, USA). Other used reagents were analytical grade, and were purchased from Sinopharmaceutical Reagents Ltd. (Shanghai, China).

Table 1. Sequences of oligonucleotides used in the experiments.

Name	Sequence (5′ to 3′)
p-DNA	Biotin-T_{10}-AGCCTATGGAATTCAGTTCTCA
f-DNA	FAM-TGAGAACTGAATTCCA
hsa-miR-146b-5p	UGAGAACUGAAUUCCAUAGGCU
hsa-miR-146a-5p	UGAGAACUGAAUUCCAUGGGUU
hsa-miR-21	UAGCUUAUCAGACUGAUGUUGA
hsa-miR-221	AGCUACAUUGUCUGCUGGGUUUC
hsa-miR-222	CUCAGUAGCCAGUGUAGAUCCU

2.2. Cell Culture and Tissue Sample Collection

Human thyroid cancer cell lines (TPC-1, K1 and C643) and human normal thyroid cell lines (Nthy-ori 3-1) were purchased from Shanghai Cell Bank, Chinese Academy of Sciences (Shanghai, China). All cells were cultured at 5% CO_2 at 37 °C in a humidified incubator (Thermo Co., Asheville, NC, USA). The PTC cell lines (K1 and TPC-1) cells were cultured in DMEM supplemented with 10% FBS and 1% penicillin–streptomycin, while the undifferentiated thyroid carcinoma cell lines (C643) and human normal thyroid cell line (Nthy-ori 3-1) were cultured in RPMI-1640 supplemented with 10% FBS and 1% penicillin–streptomycin, respectively. After full growth, the cells were digested with trypsin and counted with a Dakewe mini cell counter (Dakewe Biotech Ltd., Shenzhen, China).

Thyroid tissue collection for this work was approved by the Ethics Committee of Jilin University, and all subjects had signed informed consent prior to participating in the study. Samples were collected from 16 patients with PTC and 16 patients with nodular goiter (NG) who underwent thyroid surgery at the Thyroid Surgery department of Bethune First Hospital, Jilin University from June to July 2020, respectively. The diagnosis of each case was independently confirmed by two pathologists according to WHO classification (see Table 2 for patient details). The clinical stages were classified according to the American Joint Committee on Cancer (AJCC) tumor-lymph node metastasis (TNM) classification system. The as-obtained tissue samples were immediately stored at −80 °C until further use.

Table 2. The information of 16 papillary thyroid carcinoma (PTC) and 16 nodular goiter (NG) patients.

Patients Number	Gander	Age	Diagnosis	TNM
1	Female	30	PTC	T1aN0M0
2	Male	40	NG	/
3	Female	28	PTC	T1bN1bM0
4	Female	44	NG	/
5	Male	40	PTC	T1bN1bM0
6	Male	47	NG	/
7	Female	28	PTC	T1bN1aM0
8	Female	43	NG	/
9	Male	46	PTC	T1aN0M0
10	Male	49	NG	/
11	Female	48	PTC	T1aN0M0
12	Female	46	NG	/
13	Female	46	PTC	T1bN1aM0
14	Female	51	NG	/
15	Female	58	PTC	T1aN1aM0
16	Male	55	NG	/
17	Female	52	PTC	T1aN0M0

Table 2. *Cont.*

Patients Number	Gander	Age	Diagnosis	TNM
18	Female	51	NG	/
19	Female	55	PTC	T1aN0M0
20	Female	48	NG	/
21	Female	25	PTC	T2N1bM0
22	Female	42	NG	/
23	Male	49	PTC	T1aN1aM0
24	Female	52	NG	/
25	Female	53	PTC	T1aN1aM0
26	Female	66	NG	/
27	Male	36	PTC	T1aN1aM0
28	Female	44	NG	/
29	Male	73	PTC	T1bN1bM0
30	Male	65	NG	/
31	Female	48	PTC	T1aN1aM0
32	Male	55	NG	/

2.3. The Extraction of miRNAs

According to the manufacturer's instruction, the total RNAs of 1 mL cell solution (1×10^6 cells/mL) were extracted by the commercially available miRNA extraction kit (Qiagen Co., Inc., New York, NY, USA) in the ultra-clean platform. The extracted total RNAs were dispersed in 50 μL DEPC water. Thirty milligrams (30 mg) of thyroid pathological tissue samples were crushed and homogenized. The total RNAs of pre-treated tissue sample were extracted by the miRNA extraction kit in ultra-clean platform and re-dispersed in 50 μL DEPC water.

2.4. Preparation of MB-Probe Conjugates

The 0.2 mg M-270 MBs were resuspended in 1 mL 1 × B&W buffer, and washed three times to remove the passivator and preservative from the surface of MBs. The MBs were then collected under a magnetic frame (AMD06, Almedton Ltd., Shenzhen, China), and resuspended in 400 μL 2 × B&W buffer. Moreover, 400 μL p-DNA in various concentrations of distilled water was mixed with the MBs suspension, and incubated under gentle shaking (170 rpm) at 25 °C for 30 min. The as-obtained products (MB@ssDNA) were washed with 1 mL 1 × B&W buffer (three times) and resuspended in 400 μL reaction buffer (20 mM Tris-HCl, 150 mM NaCl, 15 mM $MgCl_2$, pH 7.0). In addition, 4 μL f-DNA (100 μM) was added into the MB@ssDNA suspension, incubated under gentle shaking (170 rpm) at 30 °C for 1 h, and washed with 1 mL reaction buffer. The final product (MB@dsDNA) was dispersed in 2 mL reaction solution for further use. The fluorescence intensity of MB@dsDNA was read by a BD ACCURI C6 flow cytometer (BD Co., New York, NY, USA).

2.5. Detection of hsa-miR-146b-5p

Five microliters hsa-miR-146b-5p in various concentrations were added into 45 μL MB@dsDNA, incubated under gentle shaking (170 rpm) at 37 °C for 1 h, and directly read by flow cytometry. In total, 10,000 MBs were recorded, and the FL1-A mean fluorescence intensity (MFI) of the MB was used for the quantitative analysis of hsa-miR-146b-5p. The content of hsa-miR-146b-5p in the tested sample was analyzed by calculating the difference value (ΔF) between the MFI of the tested sample and the blank sample. For the detection of hsa-miR-146b-5p in practical samples, 5 μL RNA extracts were added into 45 μL MB@dsDNA, incubated and detected as previously described.

3. Results

3.1. Principle of the TSDR-Based Flow Cytometric Assay

Scheme 1 shows the principle of TSDR-based flow cytometric assay for detection of PTC-related miRNA, hsa-miR-146b-5p through the TSDR on MBs. In this case, the

biotinylated probe ssDNA (p-DNA) was conjugated on the surface of the streptavidin functionalized MBs by the strong interaction of biotin with streptavidin. The carboxy-fluorescein (FAM)-labeled ssDNA (f-DNA) was then hybridized with p-DNA to prepare the fluorescent MB probe (MB@dsDNA). The MB@dsDNA is readily read by flow cytometry. After hybridization, an exposed toehold of six bases length was formed at 5′-end of p-DNA. Based on literature reports [17–23], a longer (>8 bases) toehold region will cause the instability of the hybridization of f-DNA and p-DNA, resulting in a poor detection specificity, while shorter (<5 bases) toehold region will cause a decrease in the reaction rate, resulting in a low detection sensitivity. Therefore, the toehold of six bases was used in our experiment. In the presence of hsa-miR-146b-5p, p-DNA is hybridized with hsa-miR-146b-5p through the exposed toehold region, and TSDR is initiated. The process leads to disassociate f-DNA from the surface of MBs, resulting in the decrease in the fluorescence signals of MB@dsDNA. The change of fluorescence signal of MB@dsDNA ($\Delta F = F_0 - F$, here, F_0 is the fluorescence intensity of MB@dsDNA, while F is the fluorescence intensity of MB@dsDNA after interaction with a certain amount of hsa-miR-146b-5p) is negatively dependent on the concentration of hsa-miR-146b-5p. For obtaining high detection accuracy, the average fluorescence intensity (MFI) of 10,000 MB samples was used to evaluate the concentration of hsa-miR-146b-5p.

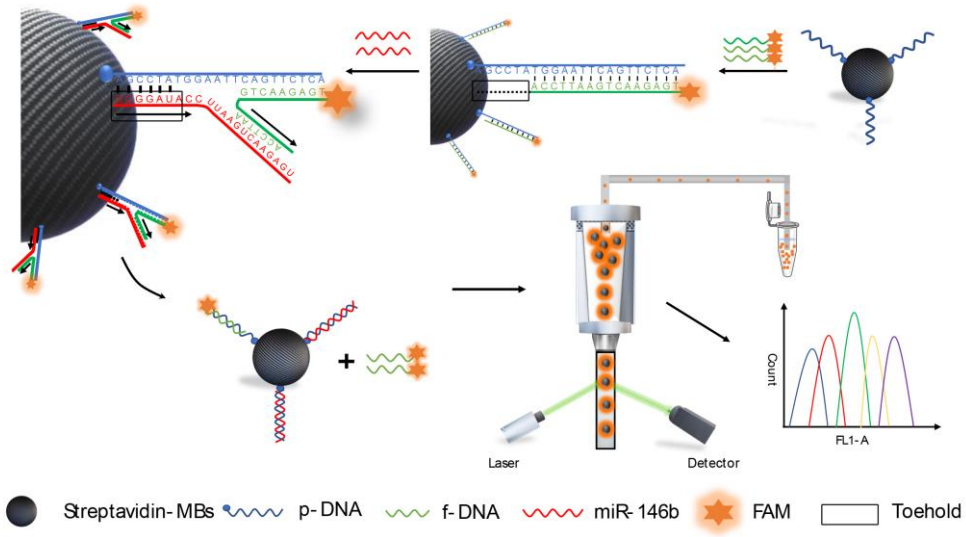

Scheme 1. The schematic illustration of the as-proposed toehold-mediated strand displacement reaction (TSDR)-based flow cytometric assay for the detection of hsa-miR-146b-5p.

3.2. Optimization of the Experimental Conditions

In order to obtain the high detection performance of hsa-miR-146b-5p, several experimental conditions were optimized including the concentration of p-DNA on the surface of MB, the reaction temperature and reaction time of MB@dsDNA with hsa-miR-146b-5p. It known that the detection efficiency of TSDR-based assays largely depend on the initial concentration of p-DNA on the surface of MBs. As shown in Figure 1, the fluorescence signal (F_0) increased with the increase in p-DNA concentration, while the concentration of MB was kept constant. However, the detection sensitivity ($\Delta F/F_0$) was decreased when the concentration of p-DNA is higher than 1 nM. In order to obtain the ideal dynamic range and the sensitivity of hsa-miR-146b-5p detection, 1 nM p-DNA was selected for the preparation of MB@dsDNA. DNA hybridization efficiency and miRNA replacement efficiency are strongly affected by reaction temperature. As shown in Figure 2, ΔF was increased by increasing the reaction temperature in the range of 27–37 °C, and obtain saturation when the reaction temperature was higher than 37 °C. Thus, 37 °C was selected as the optimal reaction temperature. To further increase assay performance, the reaction time was also optimized. As shown in Figure 3, the highest ΔF was obtained when the

MB@dsDNA was reacted with hsa-miR-146b-5p at 37 °C for 60 min. Therefore, in the following experiments, the MB@dsDNA were prepared by the reaction of 0.2 mg/mL MBs with 1 nM p-DNA, and the MB@dsDNA were reacted with hsa-miR-146b-5p at 37 °C for 60 min.

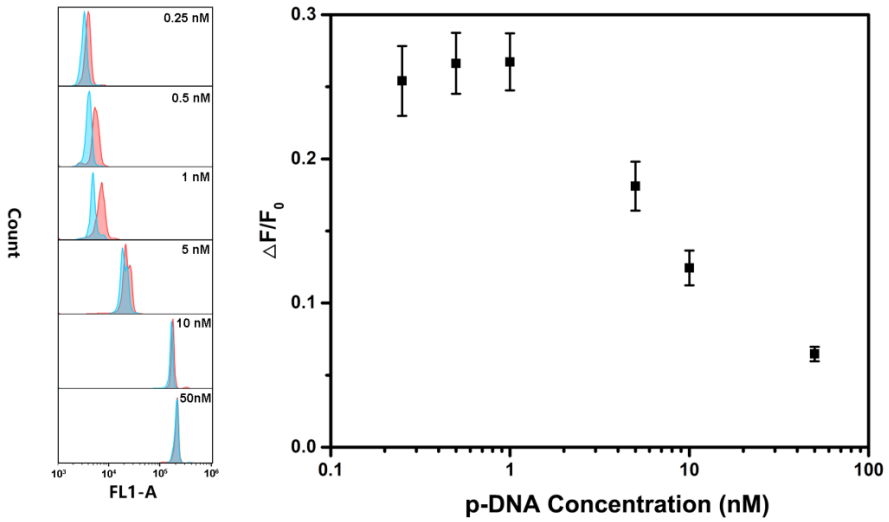

(**a**) (**b**)

Figure 1. Effect of the p-DNA concentration on the detection of hsa-miR-146-5p: (**a**) fluorescence responses of the as-prepared MB@dsDNA treated with 100 pM hsa-miR-146b-5p (blue lines) in comparison with blank control (red lines) under different p-DNA concentrations from up to down (0.25, 0.5, 1, 5, 50 and 50 nM), respectively; and (**b**) the $\Delta F/F_0$ as a function of p-DNA concentration. Error bars mean standard deviations (n = 3).

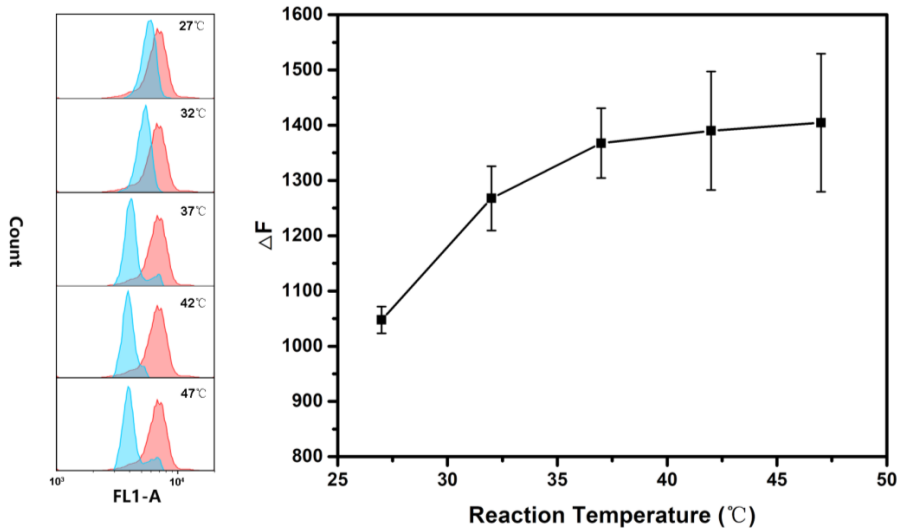

(**a**) (**b**)

Figure 2. Effect of reaction temperature on the detection of hsa-miR-146b-5p: (**a**) fluorescence responses of the MB@dsDNA treated with 100 pM hsa-miR-146b-5p (blue lines) and blank control (red lines) under different reaction temperatures (27, 32, 37, 42 and 47 °C) for 60 min, respectively; (**b**) the corresponding relative fluorescence intensity changes (ΔF) with different reaction temperatures. Error bars mean standard deviations (n = 3).

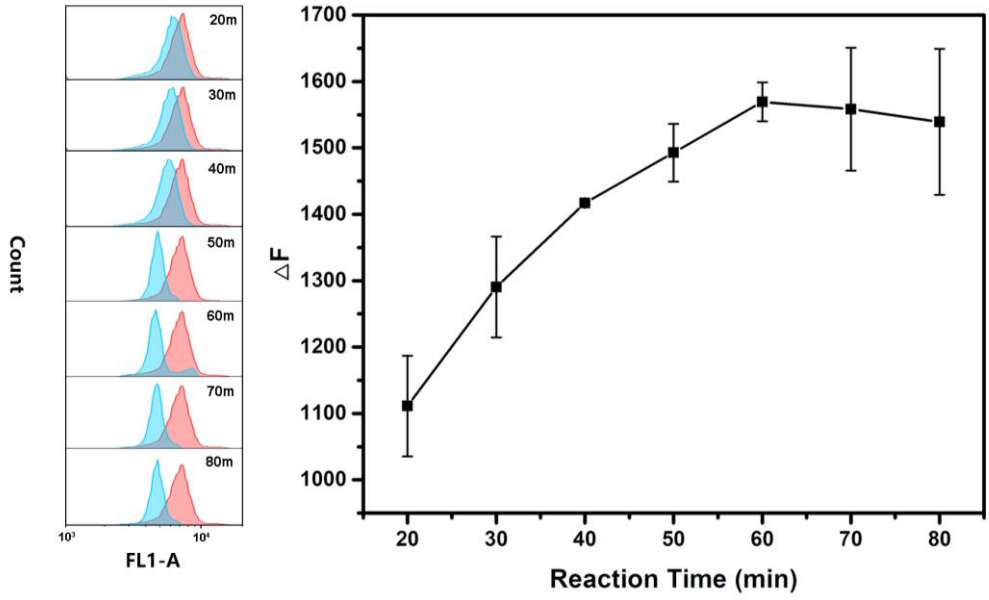

(**a**) (**b**)

Figure 3. Effect of the reaction time on the detection of hsa-miR-146b-5p: (**a**) fluorescence responses of the MB@dsDNA treated with 100 pM hsa-miR-146b-5p (blue lines) and blank control (red lines) at 37 °C under different reaction times (20, 30, 40, 50, 60, 70 and 80 min), respectively; (**b**) the corresponding relative fluorescence intensity changes (ΔF) with different reaction times. error bars mean standard deviations (n = 3).

3.3. Detection Performance of the TSDR-Based Flow Cytometric Assay

Under optimal reaction conditions, the fluorescence intensity of MB@dsDNA is decreased by increasing the concentration of hsa-miR-146b-5p (as shown in Figure 4a). It is consistent with the fact that the more hsa-miR-146b-5p exists in the solution, the more f-DNA will be dissociated from the MB@dsDNA. As shown in Figure 4b, a linear relationship between ΔF and the logarithm values of hsa-miR-146b-5p concentrations in the range of 5 pM to 5 nM is obtained. The detection limit (LOD) is estimated to be 4.21 pM according to the 3σ/S rule (σ is the standard deviation (n = 3) for the blank solution, and S is the slope of the calibration curve), which is comparable and/or better than those reported in the literature [8,39–41].

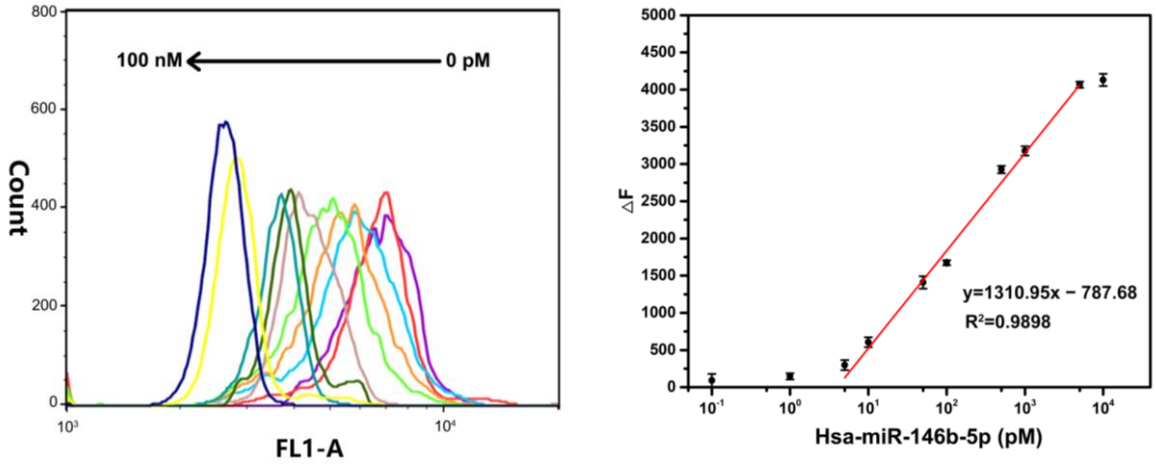

(**a**) (**b**)

Figure 4. (**a**) Fluorescence spectra and (**b**) corresponding to the data analysis of the TSDR-based flow cytometric assay towards the concentrations of hsa-miR-146b-5p ranging from 0 pM to 100 nM. Error bars mean standard deviations (n = 3).

3.4. Specificity of the TSDR-Based Flow Cytometric Assay

To address the specificity of TSDR-based flow cytometric assay, four miRNAs were used as interferences. The hsa-miR-146a-5p has similar sequence with the hsa-miR-146b-5p except for one base difference (A to G at no. 18 site). Hsa-miR-21, hsa-miR-221, and hsa-miR-222 are associated with the occurrence and development of thyroid cancer [35]. As shown in Figure 5a, the TSDR-based flow cytometric assay shows negligible ΔF towards four interferences. The experimental result indicates that the TSDR-based flow cytometric assay has good specificity.

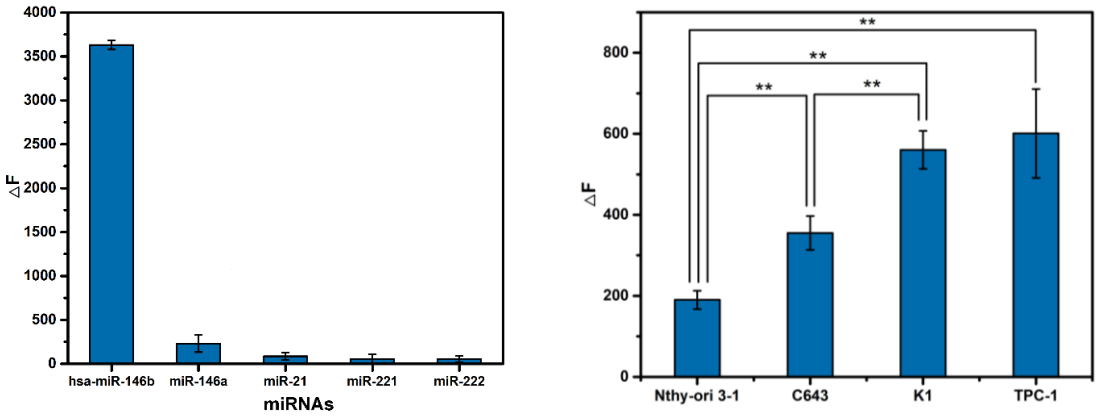

Figure 5. (**a**) Specificity of the TSDR-based flow cytometric assay. The concentrations of miRNAs are 1 nM, and (**b**) expression levels of hsa-miR-146b-5p in different cells. Error bars indicate standard deviations (n = 3, the significance of data is analyzed according to two-sided unpaired Student's t-test: ** $p < 0.01$).

3.5. Detection of Intracellular hsa-miR-146b-5p

To demonstrate its capability, the TSDR-based flow cytometric assay was applied to the profile activity levels of hsa-miR-146b-5p in different cells including two PTC cells (TPC-1 and K1), one undifferentiated thyroid cancer cell (C643) and one normal thyroid cell (Nthy-ori 3-1). The expression levels of cellular hsa-miR-146b-5p exhibit significant difference among different cells (as shown in Figure 5b), and follow the order, TPC1 ≅ K1 > C643 > Nthy-ori 3-1, which is consistent with literature-reported results [42,43], i.e., PTC cells express a higher level of hsa-miR-146b-5p than that of undifferentiated thyroid cancer cell, and normal thyroid cell expresses the lowest level of hsa-miR-146b-5p.

3.6. Detection of hsa-miR-146b-5p in Clinical Tissue Samples

For further demonstrating its applicability, the TSDR-based flow cytometric assay was used to explore the expression differences of hsa-miR-146b-5p in tissue samples from patients with PTC and/or benign thyroid lesions (NGs). In this case, 16 specimens from PTC patients and 16 specimens from NG patients were collected through the surgery. The relevant information of the patients was presented in Table 2. As shown in Figure 6a, the expression levels of hsa-miR-146b-5p in PTC tissues were significantly higher than those in NG tissues and the difference was statistically significant ($p < 0.001$), which is consistent with the reported results of relevant studies [34]. In order to prove the accuracy of this method, we drew a receiver operating characteristic curve (ROC) based on this result. The area under the ROC curve (AUC) was calculated to be 0.87 (as shown in Figure 6b). The sensitivity and specificity for the diagnosis of PTC are 81.3% and 75%, when the ΔF value is 639.01. The above results show that this method has good accuracy and practicability and has the potential to be applied in clinical practice for discriminating benign from malignant tumors. For comparison, the expression levels of hsa-miR-146b-5p in PTC tissues and NG tissues were also analyzed by qPCR method (as shown in the Figure 7). The result of TSDR-based flow cytometric assay is highly consistent with that of the qPCR analysis (as

shown in Figure 8). These results demonstrate that the TSDR-based flow cytometric assay has great promise as a practical approach that can provide high accuracy.

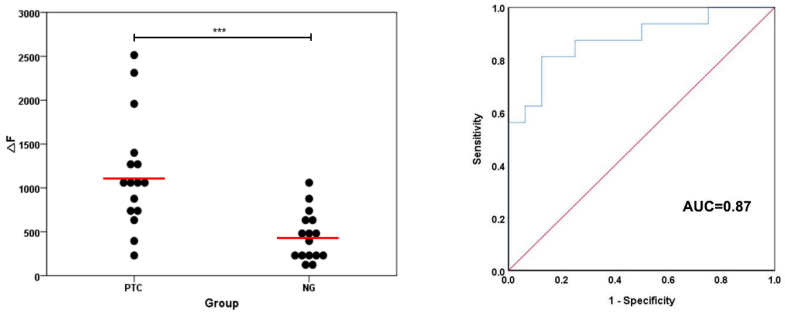

(**a**) (**b**)

Figure 6. (**a**) The expression levels of hsa-miR-146b-5p in PTC tissues and NG tissues (the significance of data is analyzed according to two-sided unpaired Student's *t*-test: *** $p < 0.001$); and (**b**) the corresponding receiver operating characteristic curve (ROC) curve generated on the basis of 32 clinical tissue samples.

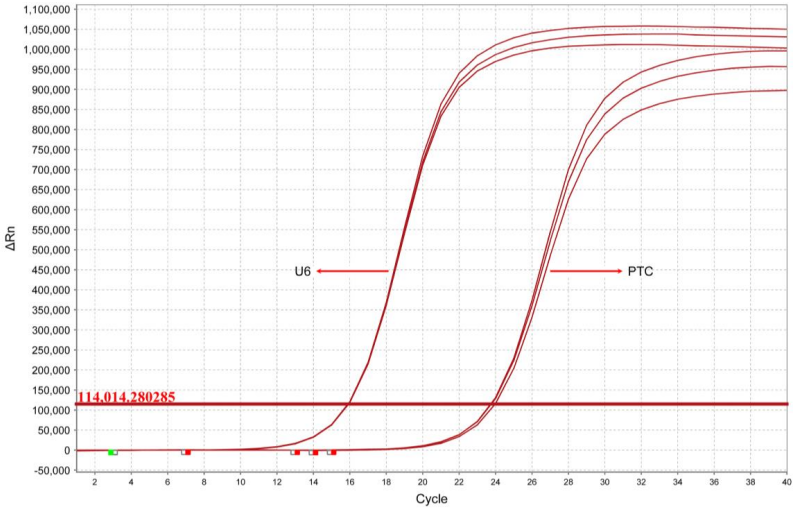

(**a**)

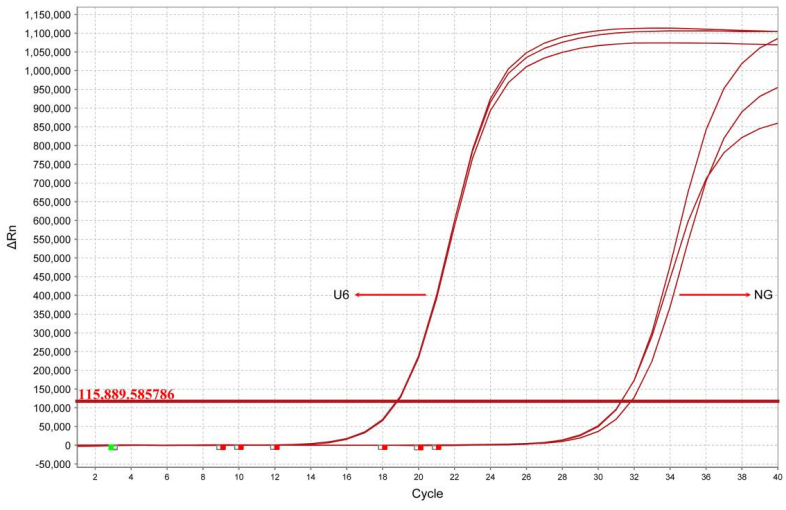

(**b**)

Figure 7. Typical qRT-PCR curves of the hsa-miR-146b-5p expressed in (**a**) PTC tissue and (**b**) NG tissue. U6 is the internal control sample.

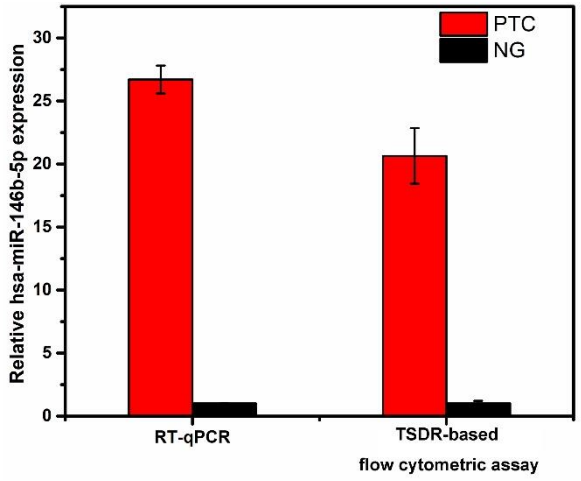

Figure 8. Relative expression levels of has-miR-146b-5p in PTC tissues and NG tissues obtained by the TSDR-based flow cytometric assay and RT-qPCR analysis. Error bars indicate the standard deviations (n = 3).

4. Conclusions

In summary, we developed an enzyme-free TSDR-based flow cytometric assay for the rapid, sensitive and selective detection of PTC-related miRNA hsa-miR-146b-5p based on the TSDR on MBs. The enzyme-free manner allows the convenient and robust detection of target miRNA with low cost. In combination with the high throughput characteristic of flow cytometry, the detection can be accomplished within 2 h except for sample preparation. In particular, the TSDR-based flow cytometric assay has been successfully employed to detect the content of hsa-miR-146b-5p in various cell lines and clinical pathological samples of PTC tissues and NG tissues. Although only hsa-miR-146b-5p is detected in the proof of principle experiment, this study provides a powerful tool for evaluating various miRNAs levels in complex matrices though changing the TSDR. Therefore, an as-proposed TSDR-based flow cytometric assay could be used as a valuable adjunctive method for improving the diagnosis accuracy of PTC because several miRNAs are significantly unregulated in PTC. In addition, with the help of existing nucleic acid enrichment techniques, our approach could be used to detect miRNAs in body fluids, which exhibits great potential in biomedical applications such as the noninvasive diagnosis of cancer.

Author Contributions: Conceptualization, X.M.; Z.W. and Y.W.; methodology, Z.W.; software, Y.W. and J.W.; validation, Y.W. and J.G.; formal analysis, Y.W. and J.W.; investigation, J.Z.; resources, Y.W. and J.Z.; data curation, Y.W. and J.G.; writing—original draft preparation, Y.W.; writing—review and editing, J.G.; visualization, Y.W.; supervision, Z.W.; project administration, X.M. and Z.W.; funding acquisition, X.M. All authors have read and agreed to the published version of the manuscript.

Funding: This research was funded by the Natural Science Foundation of Jilin Province (Theme No. 20200201357JC) and National Natural Science Foundation of China (grant No. 21974133).

Institutional Review Board Statement: This study was conducted according to the guidelines of the Declaration of Helsinki and approved by Ethics Committee of Jilin University.

Informed Consent Statement: Informed consent was obtained from all subjects involved in the study. Written informed consent has been obtained from the patients to publish this paper.

Data Availability Statement: The data presented in this study are available on request from the corresponding author.

Conflicts of Interest: The authors declare no conflict of interest.

Sample Availability: Samples of the compounds MBs and miRNAs are available from the authors.

References

1. Lee, R.C.; Feinbaum, R.L.; Ambros, V. The C. elegans heterochronic gene lin-4 encodes small RNAs with antisense complementarity to lin-14. *Cell* **1993**, *75*, 843–854. [CrossRef]
2. Bartel, D.P. MicroRNAs: Target recognition and regulatory functions. *Cell* **2009**, *136*, 215–233. [CrossRef]
3. Krol, J.; Loedige, I.; Filipowicz, W. The widespread regulation of microRNA biogenesis, function and decay. *Nat. Rev. Genet.* **2010**, *11*, 597–610. [CrossRef] [PubMed]
4. Bushati, N.; Cohen, S.M. microRNA functions. *Annu. Rev. Cell Dev. Biol.* **2007**, *23*, 175–205. [CrossRef] [PubMed]
5. Rupaimoole, R.; Slack, F.J. MicroRNA therapeutics: Towards a new era for the management of cancer and other diseases. *Nat. Rev. Drug Discov.* **2017**, *16*, 203–222. [CrossRef]
6. Hayes, J.; Peruzzi, P.P.; Lawler, S. MicroRNAs in cancer: Biomarkers, functions and therapy. *Trends Mol. Med.* **2014**, *20*, 460–469. [CrossRef] [PubMed]
7. Kosaka, N.; Iguchi, H.; Ochiya, T. Circulating microRNA in body fluid: A new potential biomarker for cancer diagnosis and prognosis. *Cancer Sci.* **2010**, *101*, 2087–2092. [CrossRef]
8. Válóczi, A.; Hornyik, C.; Varga, N.; Burgyán, J.; Kauppinen, S.; Havelda, Z. Sensitive and specific detection of microRNAs by northern blot analysis using LNA-modified oligonucleotide probes. *Nucleic Acids Res.* **2004**, *32*, e175. [CrossRef]
9. Roy, S.; Soh, J.H.; Ying, J.Y. A microarray platform for detecting disease-specific circulating miRNA in human serum. *Biosens. Bioelectron.* **2016**, *75*, 238–246. [CrossRef]
10. Chen, C.; Ridzon, D.A.; Broomer, A.J.; Zhou, Z.; Lee, D.H.; Nguyen, J.T.; Barbisin, M.; Xu, N.L.; Mahuvakar, V.R.; Andersen, M.R.; et al. Real-time quantification of microRNAs by stem-loop RT-PCR. *Nucleic Acids Res.* **2005**, *33*, e179. [CrossRef]
11. Chen, J.; Zhou, X.; Ma, Y.; Lin, X.; Dai, Z.; Zou, X. Asymmetric exponential amplification reaction on a toehold/biotin featured template: An ultrasensitive and specific strategy for isothermal microRNAs analysis. *Nucleic Acids Res.* **2016**, *44*, e130. [CrossRef]
12. Tian, W.; Li, P.; He, W.; Liu, C.; Li, Z. Rolling circle extension-actuated loop-mediated isothermal amplification (RCA-LAMP) for ultrasensitive detection of microRNAs. *Biosens. Bioelectron.* **2019**, *128*, 17–22. [CrossRef]
13. Lin, S.; Yao, G.; Qi, D.; Li, Y.; Deng, C.; Yang, P.; Zhang, X. Fast and efficient proteolysis by microwave-assisted protein digestion using trypsin-immobilized magnetic silica microspheres. *Anal. Chem.* **2008**, *80*, 3655–3665. [CrossRef] [PubMed]
14. Riahi, R.; Mach, K.E.; Mohan, R.; Liao, J.C.; Wong, P.K. Molecular detection of bacterial pathogens using microparticle enhanced double-stranded DNA probes. *Anal. Chem.* **2011**, *83*, 6349–6354. [CrossRef]
15. Zhang, Q.; Wang, F.; Zhang, H.; Zhang, Y.; Liu, M.; Liu, Y. Universal Ti(3)C(2) MXenes Based Self-Standard Ratiometric Fluorescence Resonance Energy Transfer Platform for Highly Sensitive Detection of Exosomes. *Anal. Chem.* **2018**, *90*, 12737–12744. [CrossRef] [PubMed]
16. Qiu, L.; Zhang, Y.; Liu, C.; Li, Z. A versatile size-coded flow cytometric bead assay for simultaneous detection of multiple microRNAs coupled with a two-step cascading signal amplification. *Chem. Commun.* **2017**, *53*, 2926–2929. [CrossRef] [PubMed]
17. Zhang, D.Y.; Winfree, E. Control of DNA strand displacement kinetics using toehold exchange. *J. Am. Chem. Soc.* **2009**, *131*, 17303–17314. [CrossRef] [PubMed]
18. Bi, S.; Yue, S.; Zhang, S. Hybridization chain reaction: A versatile molecular tool for biosensing, bioimaging, and biomedicine. *Chem. Soc. Rev.* **2017**, *46*, 4281–4298. [CrossRef]
19. Wang, D.; Tang, W.; Wu, X.; Wang, X.; Chen, G.; Chen, Q.; Li, N.; Liu, F. Highly selective detection of single-nucleotide polymorphisms using a quartz crystal microbalance biosensor based on the toehold-mediated strand displacement reaction. *Anal. Chem.* **2012**, *84*, 7008–7014. [CrossRef]
20. Khodakov, D.A.; Khodakova, A.S.; Linacre, A.; Ellis, A.V. Toehold-mediated nonenzymatic DNA strand displacement as a platform for DNA genotyping. *J. Am. Chem. Soc.* **2013**, *135*, 5612–5619. [CrossRef] [PubMed]
21. Zhang, J.; Wang, L.L.; Hou, M.F.; Xia, Y.K.; He, W.H.; Yan, A.; Weng, Y.P.; Zeng, L.P.; Chen, J.H. A ratiometric electrochemical biosensor for the exosomal microRNAs detection based on bipedal DNA walkers propelled by locked nucleic acid modified toehold mediate strand displacement reaction. *Biosens. Bioelectron.* **2018**, *102*, 33–40. [CrossRef] [PubMed]
22. Zhang, N.; Shi, X.M.; Guo, H.Q.; Zhao, X.Z.; Zhao, W.W.; Xu, J.J.; Chen, H.Y. Gold Nanoparticle Couples with Entropy-Driven Toehold-Mediated DNA Strand Displacement Reaction on Magnetic Beads: Toward Ultrasensitive Energy-Transfer-Based Photoelectrochemical Detection of miRNA-141 in Real Blood Sample. *Anal. Chem.* **2018**, *90*, 11892–11898. [CrossRef] [PubMed]
23. Lu, H.; Ding, B.; Tong, L.; Wu, F.; Yi, X.; Wang, J. Toehold-Mediated Strand Displacement Reaction for Dual-Signal Electrochemical Assay of Apolipoprotein E Genotyping. *Acs Sens.* **2020**, *5*, 2959–2965. [CrossRef]
24. Kong, Y.; Liu, X.; Liu, C.; Xue, Q.; Li, X.; Wang, H. A dandelion-like liposomes-encoded magnetic bead probe-based toehold-mediated DNA circuit for the amplification detection of MiRNA. *Analyst* **2019**, *144*, 4694–4701. [CrossRef] [PubMed]
25. Zhu, D.; Lu, B.; Zhu, Y.; Ma, Z.; Wei, Y.; Su, S.; Wang, L.; Song, S.; Zhu, Y.; Wang, L.; et al. Cancer-Specific MicroRNA Analysis with a Nonenzymatic Nucleic Acid Circuit. *Acs Appl. Mater. Interfaces* **2019**, *11*, 11220–11226. [CrossRef]
26. Oishi, M.; Sugiyama, S. An Efficient Particle-Based DNA Circuit System: Catalytic Disassembly of DNA/PEG-Modified Gold Nanoparticle-Magnetic Bead Composites for Colorimetric Detection of miRNA. *Small* **2016**, *12*, 5153–5158. [CrossRef] [PubMed]
27. Yue, S.; Zhao, T.; Bi, S.; Zhang, Z. Programmable strand displacement-based magnetic separation for simultaneous amplified detection of multiplex microRNAs by chemiluminescence imaging array. *Biosens. Bioelectron.* **2017**, *98*, 234–239. [CrossRef]

28. Cooper, D.S.; Doherty, G.M.; Haugen, B.R.; Kloos, R.T.; Lee, S.L.; Mandel, S.J.; Mazzaferri, E.L.; McIver, B.; Pacini, F.; Schlumberger, M.; et al. Revised American Thyroid Association management guidelines for patients with thyroid nodules and differentiated thyroid cancer. *Thyroid* **2009**, *19*, 1167–1214. [CrossRef] [PubMed]
29. Lubitz, C.C.; Sosa, J.A. The changing landscape of papillary thyroid cancer: Epidemiology, management, and the implications for patients. *Cancer* **2016**, *122*, 3754–3759. [CrossRef]
30. Haugen, B.R.; Alexander, E.K.; Bible, K.C.; Doherty, G.M.; Mandel, S.J.; Nikiforov, Y.E.; Pacini, F.; Randolph, G.W.; Sawka, A.M.; Schlumberger, M.; et al. 2015 American Thyroid Association Management Guidelines for Adult Patients with Thyroid Nodules and Differentiated Thyroid Cancer: The American Thyroid Association Guidelines Task Force on Thyroid Nodules and Differentiated Thyroid Cancer. *Thyroid* **2016**, *26*, 1–133. [CrossRef]
31. McLeod, D.S.A.; Zhang, L.; Durante, C.; Cooper, D.S. Contemporary Debates in Adult Papillary Thyroid Cancer Management. *Endocr. Rev.* **2019**, *40*, 1481–1499. [CrossRef]
32. He, H.; Jazdzewski, K.; Li, W.; Liyanarachchi, S.; Nagy, R.; Volinia, S.; Calin, G.A.; Liu, C.G.; Franssila, K.; Suster, S.; et al. The role of microRNA genes in papillary thyroid carcinoma. *Proc. Natl. Acad. Sci. USA* **2005**, *102*, 19075–19080. [CrossRef] [PubMed]
33. Abdullah, M.I.; Junit, S.M.; Ng, K.L.; Jayapalan, J.J.; Karikalan, B.; Hashim, O.H. Papillary Thyroid Cancer: Genetic Alterations and Molecular Biomarker Investigations. *Int. J. Med. Sci.* **2019**, *16*, 450–460. [CrossRef] [PubMed]
34. Chou, C.K.; Liu, R.T.; Kang, H.Y. MicroRNA-146b: A Novel Biomarker and Therapeutic Target for Human Papillary Thyroid Cancer. *Int. J. Mol. Sci.* **2017**, *18*, 636. [CrossRef] [PubMed]
35. Boufraqech, M.; Klubo-Gwiezdzinska, J.; Kebebew, E. MicroRNAs in the thyroid. *Best Pract. Res. Clin. Endocrinol. Metab.* **2016**, *30*, 603–619. [CrossRef] [PubMed]
36. Jia, M.; Shi, Y.; Li, Z.; Lu, X.; Wang, J. MicroRNA-146b-5p as an oncomiR promotes papillary thyroid carcinoma development by targeting CCDC6. *Cancer Lett.* **2019**, *443*, 145–156. [CrossRef] [PubMed]
37. Li, L.; Lv, B.; Chen, B.; Guan, M.; Sun, Y.; Li, H.; Zhang, B.; Ding, C.; He, S.; Zeng, Q. Inhibition of miR-146b expression increases radioiodine-sensitivity in poorly differential thyroid carcinoma via positively regulating NIS expression. *Biochem. Biophys. Res. Commun.* **2015**, *462*, 314–321. [CrossRef] [PubMed]
38. Riesco-Eizaguirre, G.; Wert-Lamas, L.; Perales-Patón, J.; Sastre-Perona, A.; Fernández, L.P.; Santisteban, P. The miR-146b-3p/PAX8/NIS Regulatory Circuit Modulates the Differentiation Phenotype and Function of Thyroid Cells during Carcinogenesis. *Cancer Res.* **2015**, *75*, 4119–4130. [CrossRef] [PubMed]
39. Xue, T.; Bongu, S.R.; Huang, H.; Liang, W.; Wang, Y.; Zhang, F.; Liu, Z.; Zhang, Y.; Zhang, H.; Cui, X. Ultrasensitive detection of microRNA using a bismuthene-enabled fluorescence quenching biosensor. *Chem. Commun.* **2020**, *56*, 7041–7044. [CrossRef]
40. Huang, C.H.; Huang, T.T.; Chiang, C.H.; Huang, W.T.; Lin, Y.T. A chemiresistive biosensor based on a layered graphene oxide/graphene composite for the sensitive and selective detection of circulating miRNA-21. *Biosens. Bioelectron.* **2020**, *164*, 112320. [CrossRef]
41. Park, Y.; Lee, C.Y.; Kang, S.; Kim, H.; Park, K.S.; Park, H.G. Universal, colorimetric microRNA detection strategy based on target-catalyzed toehold-mediated strand displacement reaction. *Nanotechnology* **2018**, *29*, 085501. [CrossRef] [PubMed]
42. Chou, C.K.; Chen, R.F.; Chou, F.F.; Chang, H.W.; Chen, Y.J.; Lee, Y.F.; Yang, K.D.; Cheng, J.T.; Huang, C.C.; Liu, R.T. miR-146b is highly expressed in adult papillary thyroid carcinomas with high risk features including extrathyroidal invasion and the BRAF(V600E) mutation. *Thyroid* **2010**, *20*, 489–494. [CrossRef] [PubMed]
43. Lima, C.R.; Geraldo, M.V.; Fuziwara, C.S.; Kimura, E.T.; Santos, M.F. MiRNA-146b-5p upregulates migration and invasion of different Papillary Thyroid Carcinoma cells. *BMC Cancer* **2016**, *16*, 108. [CrossRef] [PubMed]